

Visual Manipulation for Underwater Drag Force Perception in Immersive Virtual Environments

HyeongYeop Kang*
Computer Science
Department
Korea University

Geonsun Lee†
Computer Science
Department
Korea University

JungHyun Han‡
Computer Science
Department
Korea University

ABSTRACT

In this paper, we propose to reproduce drag forces in a virtual underwater environment. To this end, we first compute the drag forces to be exerted on human limbs in a physically correct way. Adopting a pseudo-haptic approach that generates visual discrepancies between the real and virtual limb motions, we compute the extent of drag forces that are applied to the virtual limbs and can be naturally perceived. Through two tests, our drag force simulation method is compared with others. The results show that our method is effective in reproducing the sense of being immersed in water. Our study can be utilized for various types of virtual underwater applications such as scuba diving training and aquatic therapy.

Index Terms: Human-centered computing—Visualization—Visualization techniques—Treemaps; Human-centered computing—Visualization—Visualization design and evaluation methods

1 INTRODUCTION

Virtual reality (VR) provides a realistic experience incorporating many types of sensory feedback. The visual feedback is often given through head-mounted displays (HMDs) which are recently being commercialized by a number of companies. However, few commercial VR products support haptic feedback, which is one of the key factors to improve the level of immersion and presence of VR experience. This is mainly because existing haptic techniques almost exclusively rely on external mechanical devices which are generally expensive and complex. As an alternative lighter approach, increasing number of studies have focused on pseudo-haptic techniques, which simulate haptic sensations exploiting phenomenon of visual dominance in human visuo-haptic integration.

Our work aims to provide a realistic underwater VR experience without using haptic devices. To this end, we focus on visual illusion determined by drag forces exerted on the users body. Therefore, we propose a pseudo-haptic approach that can reproduce the drag force without external haptic devices. More specifically, we propose to simulate the sensation of drag force by appropriately generating visual discrepancy between the real motion of the user and the virtual motion of the avatar. To this end, we employed physics equations for drag forces and conducted an experiment to identify the extent of drag forces that can be naturally perceived.

In order to verify the identified extent of drag forces, two tests were made to compare our method with others. The test results imply that our method is effective in reproducing the underwater drag force sensation. We also developed a prototype application to investigate how our technique affects the level of presence and enjoyment. Lastly, based on the lessons and insights we gained

through the user studies, we provide implementation guidelines which can help design and develop VR underwater applications.

2 RELATED WORK

The visual input in a VR application plays a major role in user experience. It is thus critical to recognize the role of visual cues among modalities. It is well-known that visual dominance exists over other multisensory inputs [32]. The ‘rubber-hand’ illusion has shown that seeing a dummy hand being brushed in synchrony with somatosensory stimulation of real hand leads to the illusion that the dummy hand has become part of real body [4]. Burns et al. [5] pointed out that, due to the visual dominance, users are more tolerant to visual proprioceptive conflict than visual interpenetration. A common use of this visual dominance is visual gains, differing the mapping ratio of the virtual movement to the real-world movement [47]. Various researches employed this to control users’ perception on speed [10,41], walking [14, 30, 36, 42], jumping [21], and head movements [15].

Taking advantage of such dominance of vision, studies have emerged on simulating haptic sensation with vision but without the haptic stimulus, known as pseudo-haptics [3, 26]. The pseudo-haptic effect of texture was provided by altering the cursor’s motion as it moved over an image [24], and also by varying the size of the cursor [25]. Dominjon et al. [7] evaluated the influence of the control/display ratio on the perception of mass using a hidden static controller and a 2D representation on a screen. Jauregui et al. [16] demonstrated how the visual animation of a self-avatar can be artificially modified in real time to create a haptic illusion of lifting weight. Rietzler et al. [39] manipulated users’ time perception in immersive virtual environments (IVEs) by applying a low pass filter on the angular velocity between a joint’s angle of the tracked user and the virtual avatar. Reitzler et al. [38] proposed to use visual tracking offsets in VR, letting users perceive weights of objects.

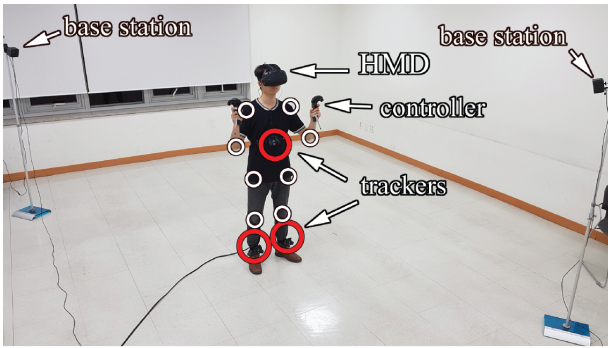
In this context, visual inputs can provide the sense of resistive force. In one of the early developments, Lécuyer et al. [23] simulated stiffness by altering the visual displacement of a virtual spring. Lécuyer et al. [27] also simulated visual stiffness of a virtual piston based on Hooke’s law. The results suggested that distorting the visual displacement can blur one’s proprioceptive perception. Rietzler et al. [37] proposed an approach to create a kinesthetic feedback by combining the tactile haptics and visual manipulations. An interesting concept, compensatory postural adjustment, was leveraged to produce the haptic illusion of a force field by Pusch et al. [35]. The visual representation of the hand was dynamically displaced along or against the virtual wind, and users were instructed to stabilize their hand. In this process of stabilization, about 70% of the subjects reported that they felt force exerted on their hand.

On the other hand, there have been attempts to reproduce the resistive force through haptic devices. GyroVR is a system that attaches flywheels on the front of an HMD to generate perpendicular force [11]. The force makes it difficult for users to move their head and enables users to perceive a sense of inertia. Nagai et al. [29] developed a wearable haptic system where wires from the motor are attached to the user’s wrists. The device provides forces for users moving virtual objects within the spatial restriction of the

*e-mail: siamiz88@gmail.com

†e-mail: g_sun@korea.ac.kr

‡e-mail: jhan@korea.ac.kr



(a)



(b)

Figure 1: Experiment setup and virtual scene. (a) Small white circles represent the joints, the angular velocities of which are reduced by drag forces. (b) Virtual underwater scenery.

wire frame. Heo et al. [12] demonstrated a hammer-shaped force feedback device that can reproduce propulsive force. However, these hardware systems are often costly and hard to implement.

The underwater movement of human being has been investigated through the past decades in the areas of physics and kinematics [17]. Kato et al. [19] conducted a comparison analysis on locomotion between underwater and land, such as walking speed, and joint angles. There have been attempts to measure such difference caused by hydrodynamic force [9, 43]. This could be useful for understanding swimming behavior [1, 40] and rehabilitation with aquatic exercise and aquatic therapy [13, 22, 34, 44].

As an effort to accurately examine hydrodynamic drag force, Berger et al. [2] investigated the drag force coefficients for the hand/arm model. Poyhonen et al. [33] also found the drag force coefficients for the knee extension-flexion movement. For the first pseudo-haptic approach to the sensation of moving in an underwater environment, we took into account these examinations in order to develop a realistic illusory sensation of underwater drag force.

3 UNDERWATER DRAG FORCE SIMULATION

The goal of our work is to induce the sensation of underwater movement with a pseudo-haptic approach. Specifically, we provide a deviation or discrepancy in the motion between the user's limb and avatar's limb.

Two major types of forces that influence an object's underwater movement are *buoyancy* and *drag*. Buoyancy is an upward force against the gravitational force. It is ever-present in an underwater environment and is perceivable without any motion. As our goal is to provide visual stimulus which is appropriately synchronized to user's motion, buoyancy is not of our interest and we will focus on drag.

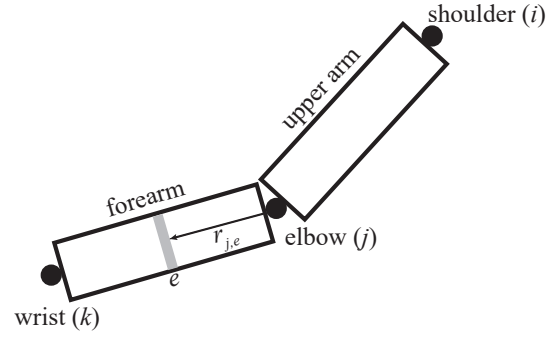


Figure 2: Shoulder, elbow, and wrist in the human skeleton's hierarchy.

3.1 Virtual Underwater Environment

In our study, we used HTC Vive headset. We set the tracking volume to 'Room-scale mode.' Its dimensions were $3.2m \times 3.2m \times 3.2m$. A user's motion was tracked with two controllers and three trackers. See Figure 1-(a). The controllers were held in both hands. A tracker was fastened around the stomach with a strap and two were attached to both ankles. Based on the tracked positions, the user's posture was computed with inverse kinematics [31]. Then, the avatar was rendered by the Unity game engine. All experiments were made in the underwater scene rendered by Unity. See Figure 1-(b). For the auditory input, the user put on earphones connected to the headset, which had an underwater bubbly sound playing on repeat.

3.2 Drag Force and Angular Velocity

Figure 2 shows part of the human skeleton's hierarchy, where the shoulder denoted as i is the parent of the elbow denoted as j , which is the parent of the wrist denoted as k . In our study, the parent-child joints are assumed to be connected by a cylindrical bone. In Figure 2, consider the forearm, which rotates about the elbow, j . By slicing the cylindrical forearm, we can define an infinitesimal volume element, e . Then, the *drag force* exerted on e , $F_{d,e}(j)$, is defined as follows [2, 33]:

$$F_{d,e}(j) = -\frac{1}{2}\rho\|\omega_j \times r_{j,e}\|^2 c_d A_e \frac{\omega_j \times r_{j,e}}{\|\omega_j \times r_{j,e}\|} \quad (1)$$

where ρ is the water density (for example, $995.7kg/m^3$ at $30^\circ C$), ω_j is the angular velocity of joint j , $r_{j,e}$ is the vector connecting j and e , c_d is the drag coefficient of human limbs, which is approximately 0.2, and A_e is the cross section of e projected to the plane perpendicular to the flow direction.

In Equation (1), the angular velocity, ω_j , is of the 'real body.' It is obtained using the Vive trackers/controllers and inverse kinematics in real time. Then, the drag force, $F_{d,e}(j)$, is applied to the same joint j of the 'avatar' to reproduce the underwater motion. Let $\Delta\omega_j^a$ denote the time evolution of joint j 's angular velocity in the avatar and $\Delta\omega_j^r$ denote that in the real body. $\Delta\omega_j^a$ and $\Delta\omega_j^r$ are related by a line integral equation:

$$\Delta\omega_j^a = \Delta\omega_j^r + \frac{\Delta t}{I_{j,k}} \int_{C_{j,k}} F_{d,e}(j) \times r_{j,e} \quad (2)$$

where Δt is the time step size, $I_{j,k}$ is the moment of inertia from j to k (wrist in the forearm example), and $C_{j,k}$ represents the line segment connecting j and k . In our study, $C_{j,k}$ is obtained by measuring each participant's body segments beforehand, and the mass required for computing $I_{j,k}$ is extracted from the report on the human body [45].

The angular velocity of the avatar's joint is reduced by drag force. With an assumption that arms move with constant acceleration,

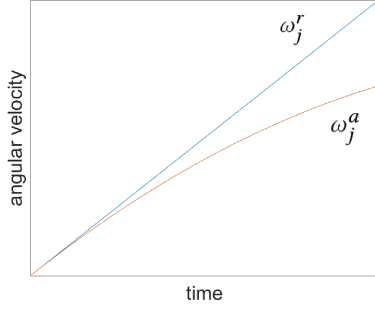


Figure 3: The angular velocity in the real body (ω_j^r) vs. that in the avatar (ω_j^a).

Figure 3 compares ω_j^a and ω_j^r . As the user moves the arm faster, the velocity difference with the avatar's arm becomes larger. If the user's arm moves too fast, the difference reaches the level where the user cannot interact with the virtual environment using the avatar's arm. Therefore, the maximum allowable difference between the real and virtual arms' orientations is empirically set to 60° in the current implementation.

Let us now consider the shoulder, i , in Figure 2. In the avatar, the time evolution of its angular velocity, $\Delta\omega_i^a$, is defined in terms of the drag forces exerted on both upper arm and forearm:

$$\Delta\omega_i^a = \Delta\omega_i^r + \frac{\Delta t}{I_{i,k}} \left(\int_{C_{i,j}} F_{d,e}(i) \times r_{i,e} + \int_{C_{j,k}} F_{d,e}(j) \times r_{i,e} \right) \quad (3)$$

where the first integral form takes into account the drag force exerted on the upper arm, and the second integral form is for the forearm.

Our current study considers four joints, which are directly related to the limb motions, i.e., shoulder and elbow for arm, and hip and knee for leg. For hip and knee, the angular velocities reduced by the drag forces are computed in the same way as in shoulder and elbow.

4 EXPERIMENT FOR DRAG FORCE

Humans accept multiple sources of sensory information and take a weighted average across the individual sensory signals [8]. Our pseudo-haptic approach solely uses the visual cue to reproduce the water's resistance to limb motions while limiting other sensory modalities. Normally, visual feedback alone is insufficient to give the sensation of being immersed in water. However, if we strengthen the visual cues we can overcome this limitation.

To this end, we increase the magnitude of drag force, which determines the visual cue. The goal of our experiment was to identify how much drag force can be applied to provide *natural* underwater sensation. For the experiment, the drag force defined in Equation (1) was multiplied by the numbers in the range of $[0.0, 6.0]$ with steps of 1.0 to define seven distinct drag-force instances. (We call these numbers *multipliers*. They were determined through a pilot test.) The set of seven multipliers was used in the experiment. Note that the multiplier, 1.0, does not change $F_{d,e}(j)$ in Equation (1) and so represents the real-world drag force.

4.1 Participants

Twenty participants (16 males and 4 females) were recruited for the experiment. The mean age was 24.25 ($SD = 2.57$) and the mean height was 171.8cm ($SD = 8.61$). All subjects had experience in aquatic activities such as swimming, diving, treading, etc. and five of them swam regularly (at least once a week). All subjects were thus familiar with the sense of hydrodynamic drag force. All had normal or corrected-to-normal vision, and fifteen had experiences

with HMD, 3D game, or 3D movie. Each subject was paid 10 USD for participation.

4.2 Method and Procedure

In the experiment, the user swings their arm horizontally. It is guided by a virtual ball, as shown in Figure 4-(a). If the ball appears on the right of a subject, the subject is instructed to stretch out the right arm toward the ball. If the ball appears on the left, the subject stretches out the left arm. Then the ball makes a horizontal semicircle (180°) about the subject's shoulder. The subject is instructed to keep their arm straight and follow the ball with their hand. During this motion, the subject is allowed to twist their upper body.

The ball takes two seconds to complete its 180° rotation. After resting for a second, it then reverses its direction along the same path and the user is instructed to also follow it with their hand. This pair of 180° back-and-forth rotations makes up a trial, which takes five seconds in total.

During a 180° rotation, the angular speed of the ball starts from 0 rad/s and is increased with a constant angular acceleration of $\pi \text{ rad/s}^2$, resulting in a slow-to-fast motion. Such a motion allows the user to experience 'increasing' drag forces. (Recall that, as presented in Equation (1), the drag force is a function of the angular velocity/speed.)

Before the experiment, each subject filled out a simple demographic survey and a body measurement was taken, for example, to determine $C_{j,k}$ in Equation (2). After a brief introduction of the task, the subject wore the HMD, trackers, and controllers to start experiment.

In the experiment, a block was composed of 10 trials, and one subject went through five blocks. There was a two-minute break between two consecutive blocks. In the first three trials of a block, the drag force was not applied at all, i.e., the multiplier was set to 0.0. The remaining seven trials were defined by seven distinct multipliers, and their order was counter-balanced between blocks. After completing each of the seven trials, the subject was asked to compare the trial's drag force with their personal underwater experience. The subject replied whether the perceived drag force was 'too weak,' 'natural,' or 'too strong.'

In our experiment, all 20 subjects were right-handed. Ten subjects were instructed to use only their right arms through the entire experiment whereas the other ten were to use their left arms. The selection of the left/right arms was randomly made.

The entire experiment took 15 to 20 minutes. Each subject filled out Simulator Sickness Questionnaire (SSQ) [20] before and after the experiment, and was also solicited for general comments.

4.3 Result and Analysis

The experiment results are depicted in Figure 5, where the x -axis is for the drag-force multiplier and the y -axis represents the probability that the multiplied drag forces are judged as 'natural.' The curve is the fitted Gaussian function of the form, $f(x) = \frac{a}{e^{-(x-b)^2/2c^2}}$ with real numbers a , b , and c . The mean (μ) is taken as the *most natural* multiplier. It is 4.05. The range of natural multipliers is defined by $\mu \pm \sigma$, where σ denotes the standard deviation. It is $[2.5, 5.6]$ as $\mu = 4.05$ and $\sigma = 1.56$.

The most natural multiplier, 4.05, implies that, in a pseudo-haptic approach, the drag force required for simulating underwater arm motions is much stronger than that of the real world. As discussed at the beginning of this section, this is ascribed to the fact that the visual cue plays a major role in reproducing the water's resistance to limb motions while other sensory modalities are limited.

As the Shapiro-Wilk and Kolmogorov-Smirnov tests at 5% significance level proved the normality, we conducted a paired t-test to see whether selection between the left and right arms affected the subjects' decisions. No significant difference was found between the two groups ($t(319) = -1.525$, $p > 0.05$).

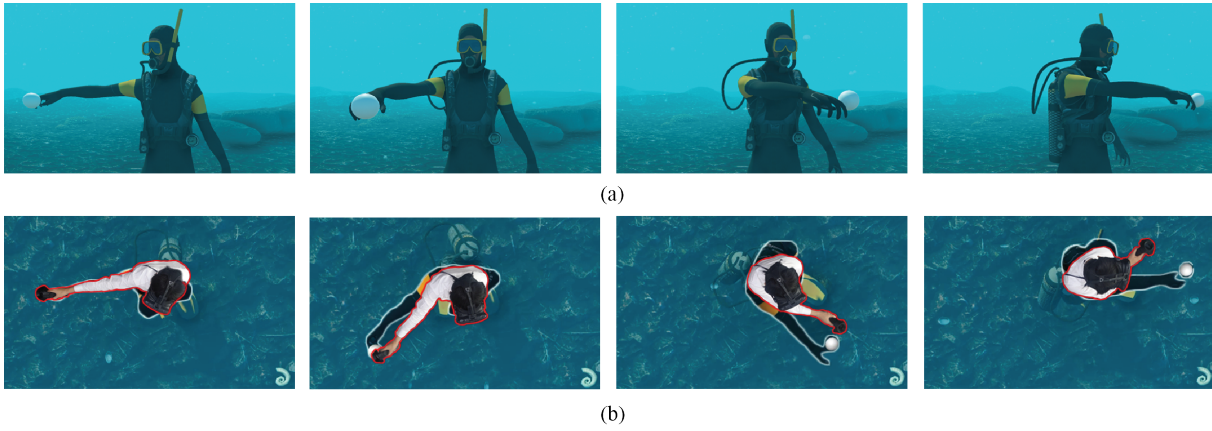


Figure 4: The forward rotation in the experiment: (a) The subject's arm follows the ball's semicircular movement [front view]. (b) Discrepancy between the real arm (in red boundary) and the virtual arm (in white boundary) [top view].

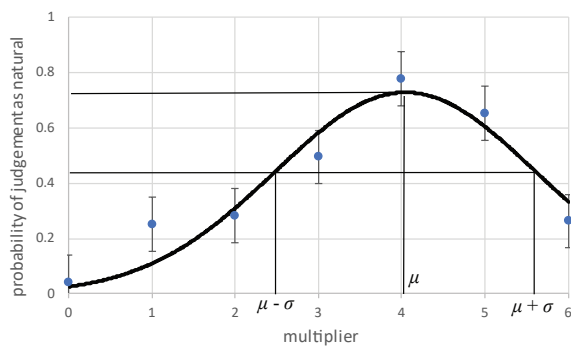


Figure 5: The experiment results.

The Shapiro-Wilk and Kolmogorov-Smirnov tests for the pre- and post-SSQs found that they were not in a normal distribution. Therefore, we performed Wilcoxon signed-rank tests and found that there was no significant difference ($Z = -0.437, p > 0.05$).

5 TEST 1: DRAG ON ARMS

In order to verify our drag-force simulation method, we made a test (henceforth named T1), where we used the most natural multiplier, 4.05, identified in Section 4. Let us call our method simply **drag force**.

To the best of our knowledge, there has been no pseudo-haptic method that recreates hydrodynamic drag force. On the other hand, visual gain is often adopted in perception studies [30, 41] as its implementation is relatively simple. A *visual gain* is defined as the ratio of the virtual-world displacement to the real-world one.

In T1, **drag force** was compared with two other methods, which we called **visual gain** and **no manipulation**:

- **visual gain**: Through a preliminary test, the visual gain was set to 0.7, i.e., the joint rotation of a subject was scaled down to 70% and then applied to the avatar's joint.
- **no manipulation**: In this method, neither drag force nor visual gain was applied to the avatar's joint. Therefore the virtual arm's motion was identical to the real arm's.

For T1, 20 subjects were re-recruited from the experiment. However, T1 was separated from the experiment by two weeks to prevent the subjects from getting used to **drag force**.

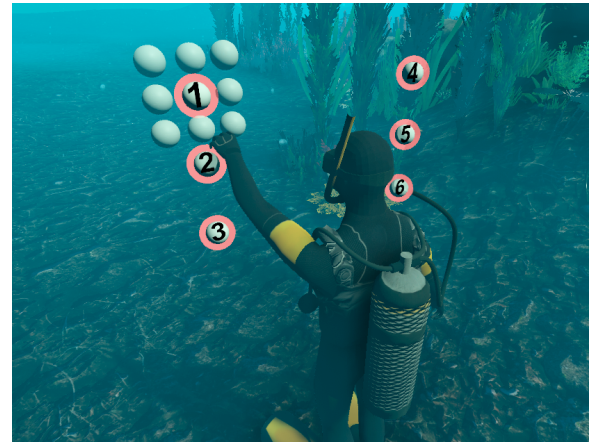


Figure 6: In **touch** task, a grid of 3×3 balls appears 60cm ahead of the subject at six different locations: 1, 2, and 3 are on the left whereas 4, 5, and 6 are on the right. Whereas 1 and 4 are above the shoulder, 2 and 5 are as high as the shoulder, and 3 and 6 are below the shoulder. Right before displaying the balls, the subject is instructed to horizontally straighten the arm to the side. This ensures that the arm moving toward the grid's center is sufficiently exposed to water's resistance.

5.1 Method and Procedure

The goal of T1 was to find which of the three methods (**drag force**, **visual gain**, and **no manipulation**) was more successful in reproducing the underwater sensation against the arm motion. T1 was composed of two tasks, **swing** and **touch**:

- **swing**: This motion was identical to that of the experiment. Guided by a ball which made a semicircle, the subject swung their arm horizontally back and forth. Such a trial was made twice with the right arm, and another two trials were made with the left arm. After four trials were completed with a method, the next method was given to the subject. The order of three methods and the selection of left/right arms were counter-balanced between subjects. The goal of **swing** task was to estimate the *sense of presence* brought by each method.
- **touch**: The goal of this task was to examine how accurately subjects could control their arms with each method. A grid of 3×3 balls was randomly displayed at six different locations, as shown in Figure 6, and the subject was instructed to touch the

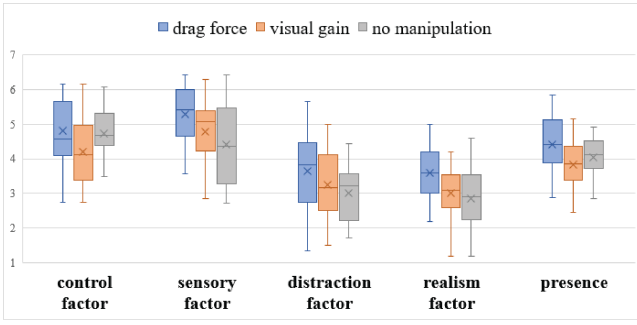


Figure 7: Responses to Witmer-Singer presence questionnaire for **swing** task. Every question was answered in a 7-point Likert scale. Shown are the median, mean, interquartile ranges, and maximum/minimum values (whiskers).

center ball. Six trials were made with the right arm, and another six were made with the left arm. A trial was judged as ‘success’ if the center ball was touched but no surrounding ball was. During a trial, the Vive controllers’ positions were tracked to compute the wrist velocities. After 12 trials were completed with a method, the next method was given to the subject. The order of three methods, the order of six locations, and the selection of left/right arms were counter-balanced between subjects.

A subject first completed **swing** task and then moved to **touch** task. Before and after each task, subjects filled out the SSQs. After completing a method for **swing** task, subjects filled out the Witmer-Singer presence questionnaire [46] and our original questionnaires listed in Table 1. There was a two-minute break between methods. After completing a method for **touch** task, subjects filled out the questionnaires in Table 1. There was a five-minute break between methods.

5.2 Results and Analysis

As the tasks of T1 took only a short period of time, none of the trials exceeded the predefined maximum deviation of 60° (presented in Section 3.2). The Witmer-Singer presence questionnaire is composed of *control*, *sensory*, *distraction* and *realism* factors, and the average of their scores represents *presence*. Figure 7 illustrates the responses for **swing** task. We used Shapiro-Wilk and Kolmogorov-Smirnov tests to find that the scores of all factors showed normal distributions.

A one-way ANOVA test revealed significant differences between the scores for sensory factor ($F(2, 57) = 3.587, p < 0.05$) and also between the scores for realism factor ($F(2, 57) = 3.587, p < 0.05$) whereas there were no significant differences in control factor, distraction factor, and presence.

For sensory factor, post hoc comparisons using the Tukey’s HSD test indicated that the mean scores in **drag force** ($\mu = 5.27, \sigma = 0.86$) were significantly different from those in **no manipulation** ($\mu = 4.42, \sigma = 1.12$). For realism factor, there was a significant difference between the mean scores in **drag force** ($\mu = 3.59, \sigma = 0.82$) and those in **no manipulation** ($\mu = 2.86, \sigma = 0.95$).

Figure 8 shows the results of analyzing the responses to our original questionnaires for **swing** task. For **realism**, a Friedman

Table 1: Our original questionnaires used in T1 and T2.

	questionnaire
Q1 (realism)	Did your motion feel realistic?
Q2 (intensity)	Was the water’s resistance intense?
Q3 (preference)	Did you like this method?

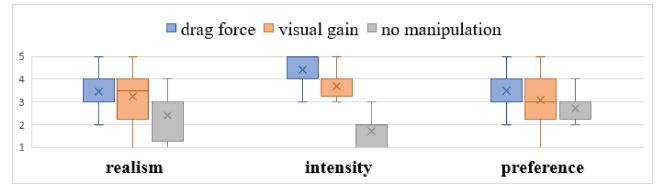


Figure 8: Responses to our original questionnaires for **swing** task (in a 5-point scale).

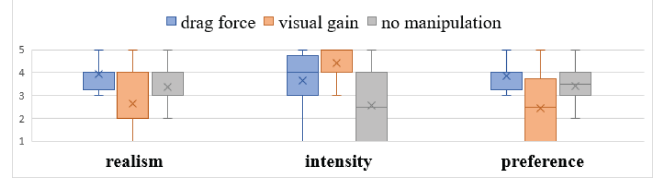


Figure 9: Responses to our original questionnaires for **touch** task (in a 5-point scale).

test, which is a non-parametric statistical test, was conducted to evaluate differences among the three methods. The test revealed that there were significant differences ($X^2(2) = 16.22, p < 0.05$). Post hoc analysis with Wilcoxon signed-rank tests was conducted with a Bonferroni correction applied, resulting in a significance level set at $p < 0.017$. There were significant differences between **drag force** and **no manipulation** ($Z = -3.137, p < 0.017$) and between **visual gain** and **no manipulation** ($Z = -2.707, p < 0.017$). However, there was no significant difference between **drag force** and **visual gain** ($Z = -0.718, p > 0.017$).

For **intensity**, there were significant differences ($X^2(2) = 35.04, p < 0.05$) among the three methods. Post hoc analysis indicated that there were significant differences between **drag force** and **visual gain** ($Z = -3.300, p < 0.017$), between **drag force** and **no manipulation** ($Z = -3.961, p < 0.017$), and between **visual gain** and **no manipulation** ($Z = -3.789, p < 0.017$).

For **preference**, there were significant differences ($X^2(2) = 11.49, p < 0.05$). Post hoc analysis indicated that there was a significant difference between **drag force** and **no manipulation** ($Z = -2.290, p < 0.017$).

We also investigated whether there was a significant difference between pre- and post-SSQs in **swing** task. The Wilcoxon signed-rank test was conducted to reveal that there was no significant difference ($Z = -0.119, p > 0.05$).

Let us now discuss **touch** task. The average wrist velocities were $0.35m/s$, $0.40m/s$, and $0.49m/s$ in **drag force**, **visual gain**, and **no manipulation**, respectively. The ‘success’ rates in **drag force**, **visual gain**, and **no manipulation** were 77%, 64%, and 84%, respectively.

Figure 9 shows the results of analyzing the responses to our original questionnaires. For **realism**, a Friedman test showed that there were significant differences ($X^2(2) = 10.983, p < 0.05$) among the three methods. Post hoc analysis with Wilcoxon signed-rank tests with a Bonferroni correction found that there was a significant difference between **drag force** and **visual gain** ($Z = -2.919, p < 0.017$).

For **intensity**, there were significant differences ($X^2(2) = 35.04, p < 0.05$). Post hoc analysis revealed that there were significant differences between **drag force** and **visual gain** ($Z = -2.944, p < 0.017$), between **drag force** and **no manipulation** ($Z = -2.915, p < 0.017$), and between **visual gain** and **no manipulation** ($Z = -3.675, p < 0.017$).

For **preference**, there were significant differences ($X^2(2) =$



Figure 10: In T2, a subject walks toward a big rock, which is 3m ahead, and then turns back to the initial position. For both forward and backward walking, the same visual gain and drag force multiplier are used. The initial position is specified by a small rock on the ground.

14.23, $p < 0.05$). Post hoc analysis revealed that there were significant differences between **visual gain** and **no manipulation** ($Z = -2.808, p < 0.017$) and between **drag force** and **visual gain** ($Z = -3.182, p < 0.017$).

Pre- and post-SSQs in **touch** task were compared by Wilcoxon signed-rank tests. There was no significant difference ($Z = -0.299, p > 0.05$).

5.3 Discussion

As can be found in Figure 7 (**swing** task), **drag force** scored the highest in every factor of the Witmer-Singer presence questionnaire. It may be worth quoting a subject’s comment made after completing **drag force**: “As the ball moved faster, my arm perceived stronger resistance of water. I felt like staying underwater.”

In **touch** task, **drag force** had the lowest wrist velocity (0.35m/s). Recall that **drag force** incurred discrepancy between real and virtual motions, as illustrated in Figure 4-(b), which usually prevented the subjects from accurately touching the target ball. In general, the slower the real motion is, the smaller the discrepancy becomes and the more accurately the target is touched. In fact, 15 out of 20 subjects commented that they slowed down their arm motion to reduce the discrepancy. This explains why the wrist velocity in **drag force** was the lowest. In **visual gain**, however, the real arm’s displacement was uniformly scaled down to 70% to define the virtual arm’s, independently of the arm’s velocity, and consequently users’ efforts to slow down their arm motion for accurately touching the target were less than those observed in **drag force**. In contrast, **no manipulation** had the highest wrist velocity. It was because there was no discrepancy between the real and virtual motions.

Similar discussions can be made for the ‘success’ rates in **touch** task. First, **no manipulation** showed the best performance because there was no discrepancy between the real and virtual motions. Second, the ‘success’ rate of **drag force** (77%) was greater than that of **visual gain** (64%) due to the effective efforts to reduce the discrepancy between the real and virtual motions. In **visual gain**, six out of 20 subjects commented that it was difficult and inconvenient to control their arms. Subjects reported that, due to such difficulty and inconvenience, they gave lower scores on realism and preference.

The results of analyzing the original questionnaire in both **swing** task (Figure 8) and **touch** task (Figure 9) show that participants gave

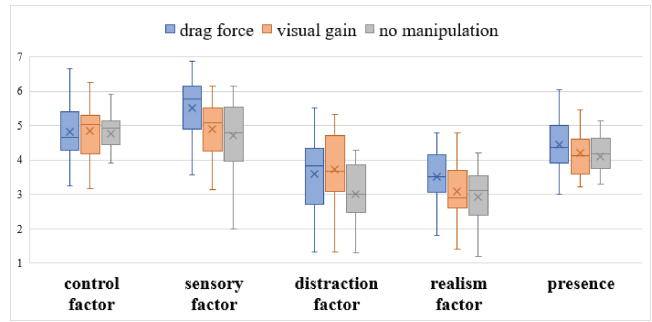


Figure 11: Responses to Witmer-Singer presence questionnaire for T2 (in a 7-point Likert scale).

more affirmative answers to **drag force**. There was no factor, where either **visual gain** or **no manipulation** excelled **drag force**.

It is worth comparing the intensity factor in **swing** task (Figure 8) with that in **touch** task (Figure 9). In **swing** task, **drag force** excels **visual gain**. However, it is not the case in **touch** task. As discussed above, users in **drag force** tended to slow down their arm motion in **touch** task. The slower the arm moves, the less resistance of water the arm perceives. As can be found in Figure 9, however, even with a lower degree of discrepancy brought by the slower motion, the sensation of water’s resistance in **drag force** is as intense as that in **visual gain**. Section 7 will discuss more on this.

6 TEST 2: DRAG ON LEGS

In the second test (henceforth, simply T2), we shifted our focus to legs’ walking motion. The most natural multiplier, 4.05, identified in the experiment was applied to the leg motion. T1 and T2 were made at the same time with the same 20 subjects. Each subject was paid 20 USD for participating in T1 and T2.

6.1 Method and Procedure

Each subject was instructed to walk 3m forward, as shown in Figure 10, and then turn back to the initial position. We took the same set of methods used in T1: **drag force**, **visual gain**, and **no manipulation**. For each method, a subject spent five minutes for training and then made three trials of back-and-forth walking. After each trial, the HMD screen faded out to black and the experimenter helped a participant to ready for a next trial. After completing a method, the subject filled out the Witmer-Singer presence questionnaire and our original questionnaires listed in Table 1. A two-minute break was between methods. In total, T2 took about 20 minutes per subject. The order of three methods was counter-balanced between subjects.

6.2 Results and Analysis

In T2, nine out of the 180 trials exceeded the maximum deviation of 60°. In such cases, the trial was discarded and subjects were asked to perform the trial again. The responses to the Witmer-Singer questionnaire are analyzed in Figure 11. The Shapiro-Wilk and Kolmogorov-Smirnov tests at the 5% revealed that the scores of all factors were normally distributed. A one-way ANOVA test revealed significant differences between the scores for sensory factor ($F(2,57) = 4.00, p < 0.05$) whereas there were no significant differences in the other four factors including presence. For the sensory factor, we performed the Tukey’s HSD test and found that the mean scores in **drag force** ($\mu = 5.51, \sigma = 0.93$) were significantly different from those in **no manipulation** ($\mu = 4.70, \sigma = 1.06$).

The results of analyzing the responses to our original questionnaires are illustrated in Figure 12, where **drag force** has the highest scores for all factors. For **realism**, a Friedman test showed that there were significant differences ($\chi^2(2) = 12.246, p < 0.05$) among

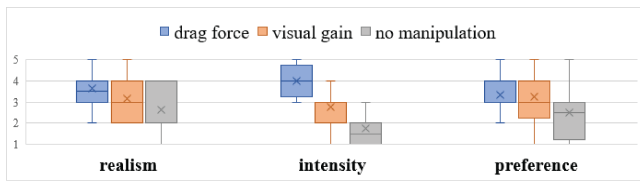


Figure 12: Responses to our original questionnaires for T2 (in a 5-point scale).

the three methods. Post hoc analysis with Wilcoxon signed-rank tests was conducted with a Bonferroni correction applied, resulting in a significance level set at $p < 0.017$. It was shown that there were significant differences between **drag force** and **no manipulation** ($Z = -2.913, p < 0.017$) and between **visual gain** and **no manipulation** ($Z = -2.762, p < 0.017$).

For **intensity**, there were significant differences among the three methods ($X^2(2) = 32.12, p < 0.05$). Post hoc analysis indicated that there were significant differences between **drag force** and **visual gain** ($Z = -3.542, p < 0.017$), between **drag force** and **no manipulation** ($Z = -3.880, p < 0.017$), and between **visual gain** and **no manipulation** ($Z = -3.245, p < 0.017$).

For **preference**, there were significant differences among the three methods ($X^2(2) = 7.559, p < 0.05$). Post hoc analysis indicated that there were significant differences between **drag force** and **no manipulation** ($Z = -2.553, p < 0.017$) and between **visual gain** and **no manipulation** ($Z = -2.543, p < 0.017$).

The positions of two Vive trackers attached to the ankles were tracked to compute the ankle velocities. The average velocities were $0.39m/s$, $0.59m/s$, and $0.60m/s$ in **drag force**, **visual gain**, and **no manipulation**, respectively. As was the case in T1, the ankle velocity in **drag force** was the lowest.

6.3 Discussion

Together with the results of analyzing the arm's **swing** task presented in Figure 7, the analysis results shown in Figure 11 indicate that **drag force** was overall more effective in providing the sense of underwater presence than **visual gain** and **no manipulation**.

Figure 12 shows that, whereas **drag force** excels **visual gain** with respect to **intensity**, it is not the case with respect to **preference**. As the real leg's velocity increases, the discrepancy with the virtual leg increases in **drag force**. In general, the leg does not move with constant velocity, and the resulting discrepancy may often make people perceive the walking motion to be unstable. (In contrast, the discrepancy in **visual gain** remains largely constant.) Obviously, the instability problem is more serious in legs than in arms. In reality, six out of 20 subjects stated that, in **drag force**, it was hard to keep the body balance while walking. A subject commented "I felt my leg motion getting deviated from my avatar's and it would soon come to a point where I couldn't walk any longer." Another commented "I couldn't keep the balance very well and so I started to walk slowly. It seemed like real underwater walking but was kind of exhausting." These explain why **drag force** does not excel **visual gain** with respect to **preference**.

The tendency to move slowly in **drag force** ($0.39m/s$) was also observed in leg movement. The discussion on the wrist velocity we made for T1 also applies here.

7 APPLICATION

Inspired by the findings in T1 and T2, which show that drag force simulation was effective in reproducing underwater sensation, we developed an application to compare three cases: (1) **drag on arms** where the drag forces are applied only to the arms, (2) **drag on limbs** where the drag forces are applied to the legs as well as to the

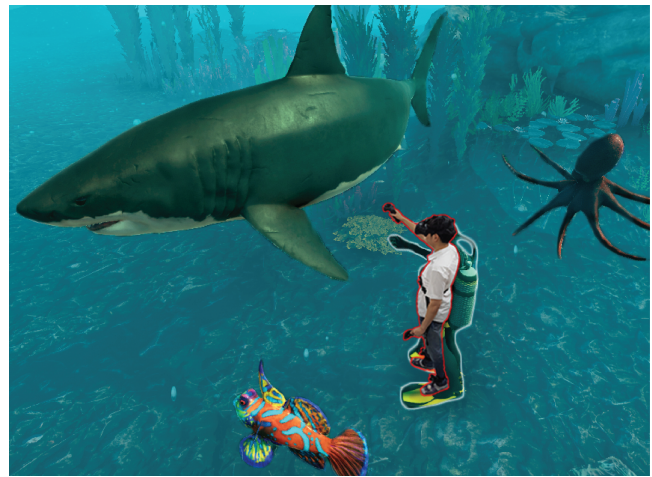


Figure 13: Underwater scene: Arm motions of the user (in red boundary) and avatar (in white boundary).

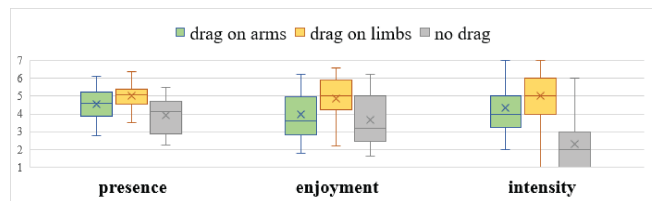


Figure 14: Responses to questionnaires for application. The questions in E²I were answered in a 7-point Likert scale and the last question was in 7 points.

arms, and (3) **no drag** where the drag forces are applied to neither arms nor legs.

For the application, 28 subjects (17 males and 11 females) were recruited. The mean age was 25.18 ($SD = 3.17$) and the mean height was $169.2cm$ ($SD = 9.33$). All subjects had experience in aquatic activities such as swimming, diving, treading, etc. and six of them swam regularly (at least once a week). All had normal or corrected-to-normal vision, 20 subjects had experiences with HMD or 3D game, and 22 subjects had experiences in 3D movie. Each subject was paid 10 USD for participation.

7.1 Method and Procedure

To the same underwater environment used for T1 and T2, we added three creatures, a shark, a fish, and an octopus. See Figure 13. A ball was attached to each creature. Its color changes if touched. Subjects were instructed to approach and touch the creatures in a given order. Touching the three makes up a trial.

Three cases of **drag on arms**, **drag on limbs**, and **no drag** were tested one by one. The order of the cases was counter-balanced between subjects. For each case, a subject spent five minutes for training and then made three trials. The order of touching three creatures was counter-balanced between cases. After completing a case, subjects filled out the E²I questionnaire [28] for investigating presence and enjoyment and an additional question asking "Was the water's resistance intense?" (henceforth, **intensity**). A three-minute break was given between cases. In total, a subject spent about 20 minutes.

7.2 Results and Analysis

The analysis results with respect to presence, enjoyment, and intensity are illustrated in Figure 14. The Shapiro-Wilk and

Kolmogorov-Smirnov tests revealed that the scores of presence, enjoyment, and intensity were normally distributed.

A one-way ANOVA test showed significant differences between the scores for presence ($F(2, 81) = 19.606, p < 0.05$). Post hoc comparisons using the Tukey's HSD test found that there were significant differences among the three cases.

For enjoyment, there were significant differences ($F(2, 81) = 8.956, p < 0.05$). Post hoc analysis indicated that there were significant differences between **drag on arms** and **drag on limbs**, and also between **drag on limbs** and **no drag**.

For intensity, there were significant differences ($F(2, 81) = 81.496, p < 0.05$). Post hoc analysis indicated that there were significant differences among the three cases.

7.3 Discussion

Section 7.2 shows that presence, enjoyment, and intensity were all increased as drag forces were applied to more limbs. Considering that several participants complained of being exhausted in T2, where the drag forces were applied to legs, it is a noteworthy fact that enjoyment scored the highest in **drag on limbs**. It may be partly due to the entertaining content of approaching and touching dynamic sea creatures. A subject commented "This was like a game and I became excited when I successfully touched the shark after getting over the water's resistance." Out of 28 subjects, 18 stated that the underwater sensation was more realistic in **drag on limbs**.

Figure 14 shows that **drag on limbs** excels the other cases with respect to intensity. This implies that, as discussed in Section 5, the resistance of water is sufficiently perceived even with a lower degree of discrepancy brought by the slower motion. Based on the subjects' comments collected from the post-experiment interview, we presumed as follows: In the application, the underwater scene was fairly realistic, as can be found in Figure 13. It was compatible with the users' underwater experience, making them take their slow limb motion as a natural consequence of being and walking underwater.

8 IMPLEMENTATION GUIDELINES

While conducting the user studies with drag force simulation, we collected limitations of our approach and also gained insights that can be provided as implementation guidelines for developing VR underwater applications:

- **Fatigue control:** As stated before, users made an extra effort to keep the body balance while walking. Worse still, unlike in a real underwater environment, users' limbs were not supported by buoyancy. Therefore, after an extended period of use, their limbs began to feel heavy, making the users quickly exhausted. A simple solution to this fatigue problem would be either reducing duration of use for an activity or providing a sufficient amount of break between activities. A serious solution would be to integrate the proposed method into a supporting apparatus such as a suspension system that can provide buoyancy.
- **Limited deviation:** If the real body motion is overly deviated from the avatar's virtual motion, users may not be able to make natural limb motions, resulting in decreased sense of presence. This problem can be prevented by defining maximum deviation of the joint angle, as we implemented and presented in Section 3. Slightly decreasing the deviation over time without users' noticing can also be a possible solution [35].
- **Task design:** A notable observation made in our study, especially in T1 presented in Section 5, is that people tended to slow down their motion when performing a task that requires accuracy. The user experiences in terms of realism, intensity, and preference varied depending on the types of tasks user performed. This implies that, with an elaborate design of the tasks or missions in an application, the sense of underwater presence may be significantly increased.

9 CONCLUSION AND FUTURE WORK

We presented a pseudo-haptic approach for inducing drag force sensation in underwater virtual environments. In order to provide a realistic sensation, we adopted physics-based drag force equations and identified the extent of drag force that can be naturally perceived. We found that the amount of drag force to be applied to the avatar limbs should be significantly amplified. We conducted two tests to compare our method with others. We also developed a VR application and collected user feedback. It was found that the underwater VR application built upon our method provides a significantly better experience than those without drag force simulation.

Our study can be utilized for various types of VR underwater applications such as scuba diving training and aquatic therapy. Furthermore, by simply altering the parameters in the drag force equation, our approach could simulate different types of drag force, e.g., wind force. On the other hand, since our approach does not require any external mechanical devices, it can be easily integrated with other systems. A possible scenario is to combine our drag force simulation with a cable- or wire-based suspension system [6, 18] that provides buoyancy.

ACKNOWLEDGMENTS

This work was supported by the National Research Foundation of Korea (NRF) Grant funded by the Korea government (MSIT) (NRF-2017M3C4A7066316 and No. NRF2016-R1A2B3014319). We would like to thank Seung-wook Kim and Min Hyung Kee for discussions on physics modeling, JunYeup Cho for assistance in developing the underwater application, and Paul C. Gloumeau for proofreading the manuscript.

REFERENCES

- [1] R. M. Alexander and G. Goldspink. *Mechanics and energetics of animal locomotion*. Chapman and Hall, 1977.
- [2] M. A. Berger, G. de Groot, and A. P. Hollander. Hydrodynamic drag and lift forces on human hand/arm models. *Journal of Biomechanics*, 28(2):125–133, 1995.
- [3] F. Biocca, J. Kim, and Y. Choi. Visual touch in virtual environments: An exploratory study of presence, multimodal interfaces, and cross-modal sensory illusions. *Presence: Teleoperators & Virtual Environments*, 10(3):247–265, 2001.
- [4] M. Botvinick and J. Cohen. Rubber hands 'feel' touch that eyes see. *Nature*, 391(6669):756, 1998.
- [5] E. Burns, S. Razzaque, A. T. Panter, M. C. Whitton, M. R. McCallus, and F. P. Brooks. The hand is slower than the eye: A quantitative exploration of visual dominance over proprioception. In *Virtual Reality, 2005. Proceedings. VR 2005. IEEE*, pp. 3–10. IEEE, 2005.
- [6] T. Cunningham. System requirements document for the active response gravity offload system (argos). *NASA Engineering directorate document AR&SD-08007*, 2010.
- [7] L. Dominjon, A. Lécuyer, J.-M. Burkhardt, P. Richard, and S. Richir. Influence of control/display ratio on the perception of mass of manipulated objects in virtual environments. In *Virtual Reality, 2005. Proceedings. VR 2005. IEEE*, pp. 19–25. IEEE, 2005.
- [8] M. O. Ernst. A bayesian view on multimodal cue integration. *Human body perception from the inside out*, 131:105–131, 2006.
- [9] B. W. Evans, K. J. Cureton, and J. W. Purvis. Metabolic and circulatory responses to walking and jogging in water. *Research Quarterly. American Alliance for Health, Physical Education and Recreation*, 49(4):442–449, 1978.
- [10] J. A. Groeger, O. M. Carsten, E. Blana, and A. H. Jamson. Speed and distance estimation under simulation conditions. *Vision in vehicles*, 7:291–299, 1999.
- [11] J. Gugenheimer, D. Wolf, E. R. Eiriksson, P. Maes, and E. Rukzio. Gyrov: Simulating inertia in virtual reality using head worn flywheels. In *Proceedings of the 29th Annual Symposium on User Interface Software and Technology*, pp. 227–232. ACM, 2016.
- [12] S. Heo, C. Chung, G. Lee, and D. Wigdor. Thor's hammer: An ungrounded force feedback device utilizing propeller-induced propulsive

- force. In *Proceedings of the 2018 CHI Conference on Human Factors in Computing Systems*, p. 525. ACM, 2018.
- [13] R. S. Hinman, S. E. Heywood, and A. R. Day. Aquatic physical therapy for hip and knee osteoarthritis: results of a single-blind randomized controlled trial. *Physical therapy*, 87(1):32–43, 2007.
- [14] A. Ishii, I. Suzuki, S. Sakamoto, K. Kanai, K. Takazawa, H. Doi, and Y. Ochiai. Optical marionette: Graphical manipulation of human’s walking direction. In *Proceedings of the 29th Annual Symposium on User Interface Software and Technology*, pp. 705–716. ACM, 2016.
- [15] P. Jaekl, M. Jenkin, and L. R. Harris. Perceiving a stable world during active rotational and translational head movements. *Experimental brain research*, 163(3):388–399, 2005.
- [16] D. A. G. Jauregui, F. Argelaguet, A.-H. Olivier, M. Marchal, F. Multon, and A. Lécuyer. Toward “pseudo-haptic avatars”: Modifying the visual animation of self-avatar can simulate the perception of weight lifting. *IEEE transactions on visualization and computer graphics*, 20(4):654–661, 2014.
- [17] K. Kaneda, H. Wakabayashi, D. Sato, and T. Nomura. Lower extremity muscle activity during different types and speeds of underwater movement. *Journal of physiological anthropology*, 26(2):197–200, 2007.
- [18] H. Kang, G. Lee, S. Kwon, O. Kwon, S. Kim, and J. Han. Flotation simulation in a cable-driven virtual environment—a study with parasailing. In *Proceedings of the 2018 CHI Conference on Human Factors in Computing Systems*, p. 632. ACM, 2018.
- [19] T. Kato, S. Onishi, and K. Kitagawa. Kinematical analysis of underwater walking and running. *Sports Medicine, Training and Rehabilitation*, 10(3):165–182, 2001.
- [20] R. S. Kennedy, N. E. Lane, K. S. Berbaum, and M. G. Lilienthal. Simulator sickness questionnaire: An enhanced method for quantifying simulator sickness. *The international journal of aviation psychology*, 3(3):203–220, 1993.
- [21] M. Kim, S. Cho, T. Q. Tran, S.-P. Kim, O. Kwon, and J. Han. Scaled jump in gravity-reduced virtual environments. *IEEE Transactions on Visualization & Computer Graphics*, (4):1360–1368, 2017.
- [22] K. Kong, H. Moon, B. Hwang, D. Jeon, and M. Tomizuka. Robotic rehabilitation treatments: Realization of aquatic therapy effects in exoskeleton systems. In *Robotics and Automation, 2009. ICRA’09. IEEE International Conference on*, pp. 1923–1928. IEEE, 2009.
- [23] A. Lécuyer, J.-M. Burkhardt, S. Coquillart, and P. Coiffet. “boundary of illusion”: an experiment of sensory integration with a pseudo-haptic system. In *Virtual Reality, 2001. Proceedings. IEEE*, pp. 115–122. IEEE, 2001.
- [24] A. Lécuyer, J.-M. Burkhardt, and L. Etienne. Feeling bumps and holes without a haptic interface: the perception of pseudo-haptic textures. In *Proceedings of the SIGCHI conference on Human factors in computing systems*, pp. 239–246. ACM, 2004.
- [25] A. Lécuyer, J.-M. Burkhardt, and C.-H. Tan. A study of the modification of the speed and size of the cursor for simulating pseudo-haptic bumps and holes. *ACM Transactions on Applied Perception (TAP)*, 5(3):14, 2008.
- [26] A. Lécuyer, S. Coquillart, A. Kheddar, P. Richard, and P. Coiffet. Pseudo-haptic feedback: Can isometric input devices simulate force feedback? In *Virtual Reality, 2000. Proceedings. IEEE*, pp. 83–90. IEEE, 2000.
- [27] A. Lécuyer, S. Coquillart, and P. Coiffet. Simulating haptic information with haptic illusions in virtual environments. Technical report, ANATOLE LÉCUYER SURESNES (FRANCE) AEROSPATIALE MATRA CCR, 2001.
- [28] J.-W. Lin, H. B.-L. Duh, D. E. Parker, H. Abi-Rached, and T. A. Furness. Effects of field of view on presence, enjoyment, memory, and simulator sickness in a virtual environment. In *Virtual Reality, 2002. Proceedings. IEEE*, pp. 164–171. IEEE, 2002.
- [29] K. Nagai, S. Tanoue, K. Akahane, and M. Sato. Wearable 6-dof wrist haptic device spidar-w. In *SIGGRAPH Asia 2015 Haptic Media And Contents Design*, p. 19. ACM, 2015.
- [30] N. C. Nilsson, S. Serafin, and R. Nordahl. Establishing the range of perceptually natural visual walking speeds for virtual walking-in-place locomotion. *IEEE transactions on visualization and computer graphics*, 20(4):569–578, 2014.
- [31] R. P. Paul. *Robot manipulators: mathematics, programming, and control: the computer control of robot manipulators*. Richard Paul, 1981.
- [32] M. I. Posner, M. J. Nissen, and R. M. Klein. Visual dominance: an information-processing account of its origins and significance. *Psychological review*, 83(2):157, 1976.
- [33] T. Pöyhönen, K. L. Keskinen, A. Hautala, and E. Mätkiä. Determination of hydrodynamic drag forces and drag coefficients on human leg/foot model during knee exercise. *Clinical biomechanics*, 15(4):256–260, 2000.
- [34] W. E. Prentice and M. L. Voight. *Techniques in musculoskeletal rehabilitation*. McGraw-Hill, 2001.
- [35] A. Pusch, O. Martin, and S. Coquillart. Hemp-hand-displacement-based pseudo-haptics: a study of a force field application. In *3D User Interfaces, 2008. 3DUI 2008. IEEE Symposium on*, pp. 59–66. IEEE, 2008.
- [36] S. Razaque, Z. Kohn, and M. C. Whitton. Redirected walking. In *Proceedings of EUROGRAPHICS*, vol. 9, pp. 105–106. Citeseer, 2001.
- [37] M. Rietzler, F. Geiselhart, J. Frommel, and E. Rukzio. Conveying the perception of kinesthetic feedback in virtual reality using state-of-the-art hardware. In *Proceedings of the 2018 CHI Conference on Human Factors in Computing Systems*, p. 460. ACM, 2018.
- [38] M. Rietzler, F. Geiselhart, J. Gugenheimer, and E. Rukzio. Breaking the tracking: Enabling weight perception using perceivable tracking offsets. In *Proceedings of the 2018 CHI Conference on Human Factors in Computing Systems*, p. 128. ACM, 2018.
- [39] M. Rietzler, F. Geiselhart, and E. Rukzio. The matrix has you: realizing slow motion in full-body virtual reality. In *Proceedings of the 23rd ACM Symposium on Virtual Reality Software and Technology*, p. 2. ACM, 2017.
- [40] R. Schleihauf Jr. A hydrodynamic analysis of swimming propulsion. *Swimming*, pp. 70–109, 1979.
- [41] G. Semb. Scaling automobile speed. *Perception & Psychophysics*, 5(2):97–101, 1969.
- [42] F. Steinicke, G. Bruder, J. Jerald, H. Frenz, and M. Lappe. Estimation of detection thresholds for redirected walking techniques. *IEEE transactions on visualization and computer graphics*, 16(1):17–27, 2010.
- [43] Y. Sugajima, G. Mitarai, M. Koeda, and T. Moritani. Characteristic changes of motor unit activity in hip joint flexor muscles during voluntary isometric contraction during water immersion. *Journal of Electromyography and Kinesiology*, 6(2):83–95, 1996.
- [44] M. A. Towler, R. J. Goitz, R. P. Wilder, L. P. Buschbacher, R. F. Morgan, and J. G. Thacker. Bioengineering principles of hydrotherapy. *The Journal of burn care & rehabilitation*, 8(6):579–584, 1987.
- [45] A. Tözeren. *Human body dynamics: classical mechanics and human movement*. Springer Science & Business Media, 1999.
- [46] B. G. Witmer and M. J. Singer. Measuring presence in virtual environments: A presence questionnaire. *Presence*, 7(3):225–240, 1998.
- [47] R. Zhang and S. A. Kuhl. Human sensitivity to dynamic rotation gains in head-mounted displays. In *Proceedings of the ACM Symposium on Applied Perception*, pp. 71–74. ACM, 2013.